

Identifying a forward scattering superconductor through pump-probe spectroscopy

Ankit Kumar,^{1,*} S. Johnston,² and A. F. Kemper^{1,†}

¹*Department of Physics, North Carolina State University, Raleigh, North Carolina 27695, USA*

²*Department of Physics and Astronomy, The University of Tennessee, Knoxville, Tennessee 37996, USA*

Electron-boson scattering that is peaked in the forward direction has been suggested as an essential ingredient for enhanced superconductivity observed in FeSe monolayers. Here, we study the superconducting state of a system dominated by forward scattering in the time-domain and contrast its behavior against the standard isotropic BCS case for both s - and d -wave symmetries. An analysis of the electron's dynamics in the pump-driven non-equilibrium state reveals that the superconducting order in the forward-focused case is robust and persistent against the pump-induced perturbations. The superconducting order parameter also exhibits a non-uniform melting in momentum space. We show that this behavior is in sharp contrast to the isotropic interaction case and propose that time-resolved approaches are a potentially powerful tool to differentiate the nature of the dominant coupling in correlated materials.

The discovery of enhanced superconductivity in FeSe intercalates [1] and ultra thin films of FeSe grown on oxide substrates [2], has attracted considerable interest. In these systems, significant electron doping drives the Γ -centered hole bands below the Fermi level E_F [3]. At face value, this Fermi surface topology challenges the picture of s_{\pm} pairing mediated by spin fluctuations enhanced by Fermi surface nesting [4]. Motivated by this, several alternative proposals have been advanced, including contributions from the so-called incipient hole band below E_F [5–7]; or from some other bosonic mode such as nematic fluctuations [8] or phonons [2, 9–13]. In particular, a unique cross interfacial electron-phonon (e -ph) coupling has been invoked to explain the higher T_c values observed in FeSe films grown on oxide substrates in comparison to the doped FeSe intercalates [10, 11, 14, 15]; this interpretation, however, is controversial [16–21], and finding experimental probes that might provide new insight into this problem is imperative.

A common feature of the scenarios based on nematic fluctuations or cross-interface e -ph coupling is the importance of forward scattering, where the relevant electron-boson coupling constant is peaked strongly at small momentum transfers \mathbf{q} . Such a momentum structure can have significant consequences for superconductivity [12, 22–24], enhancing pre-existing superconductivity in unconventional pairing channels, or resulting in significant T_c values if the interaction is sufficiently peaked around $\mathbf{q} = 0$ [10, 12, 22, 24–26]. These results naturally raise the question: how can one uniquely identify superconductivity mediated by a forward-focused interaction?

We address this issue in this Letter by studying the problem in the time-domain. We consider superconductivity mediated by an optical phonon in the idealized perfect forward scattering limit (i.e. a delta-function coupling) and contrast its behavior to the case where superconductivity is mediated by an isotropic interaction. (While we adopt a phonon mode for simplicity, our results are also applicable to the pairing mediated by nematic fluctuations.) In both cases, we drive the sys-

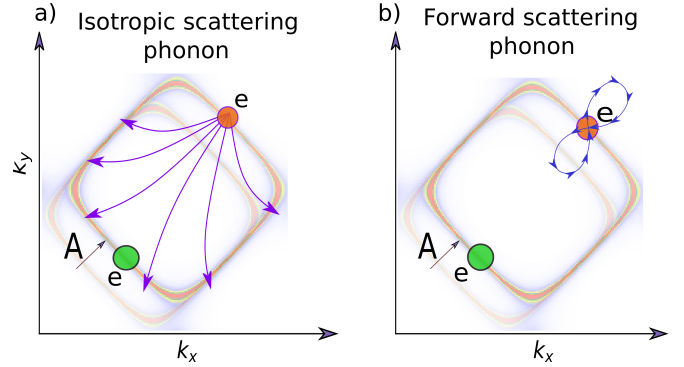


FIG. 1. (Color online) An illustration of the allowed scattering processes in the system, where the Fermi surface is displaced by a pump $\mathbf{A}(t)$ applied along the (11) direction. **a)** Scattering of electrons by isotropically coupled optical phonons. The electron may scatter to all allowed \mathbf{k} states. **b)** Scattering of electrons by optical phonons with a bias towards the forward scattering. The electron has restricted phase space available to scatter to other states.

tem into a non-equilibrium state by an ultrafast pump pulse and study the properties of the transient non-equilibrium state. We find that the two interactions show significant contrasting behavior in spectroscopic measurements. First, the suppression of the superconducting order in the isotropic case shows a strong dependence on the pump fluence. The forward scattering superconducting state is comparatively robust against pump-induced suppression. The energy absorption is also much smaller in the forward focused case. Second, while the suppression of the superconducting gap in the isotropic case is uniform in momentum space, the forward scattering shows a specific momentum-dependent suppression of the gap. This particular contrasting behavior can be measured in momentum- and time-resolved measurements, such as trARPES, and can provide evidences to either validate or falsify the forward scattering mechanism in FeSe monolayers.

The observed effects can be understood as a direct con-

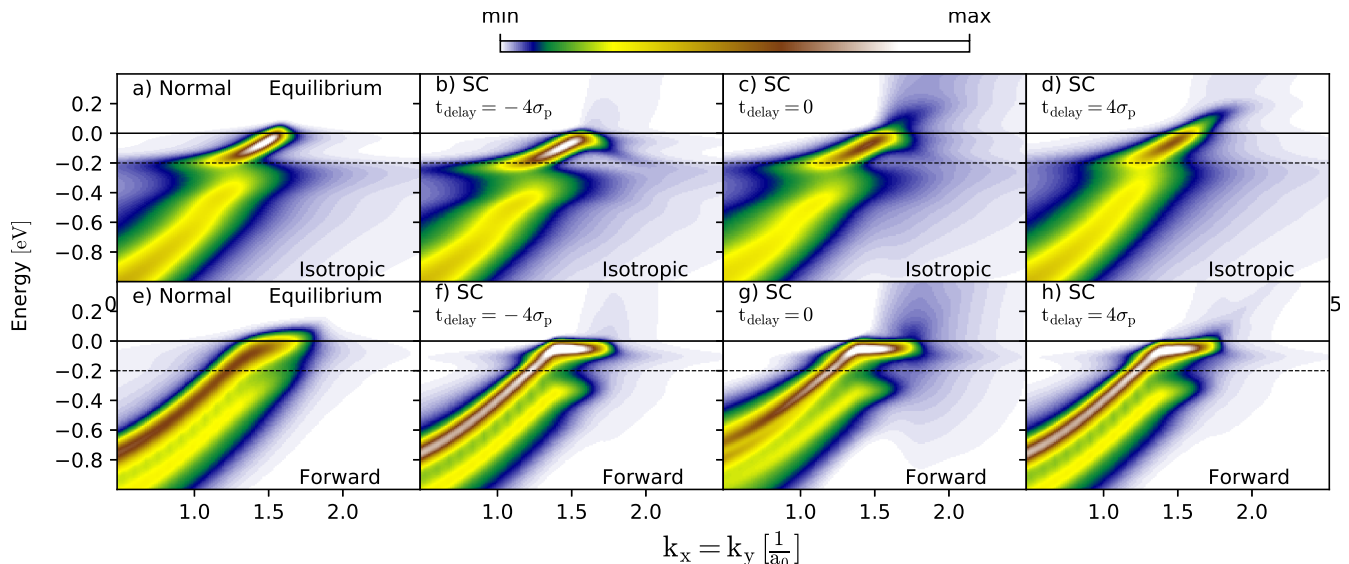


FIG. 2. (Color online) tr-ARPES spectra of the isotropic scattering and the forward scattering along the (1,1) direction for s -wave pairing symmetry. Panels **a** and **e** display the equilibrium normal state. The Fermi energy (E_F) and phonon frequency are shown by the solid horizontal line and dashed line respectively. Panels **b-d** and **f-h** show the time-resolved ARPES spectra of the superconducting state when a pump pulse drives the system out of equilibrium.

sequence of the *restricted phase space* available to scattering process in the forward scattering case. Figure 1 shows schematic scattering processes at E_F , where electrons are driven by an ultrafast pump field $\mathbf{A}(t)$. In the case of an isotropic e -ph interaction, an electron can scatter to all energy and momentum conserving eigenstates. In contrast, in the forward focused case, the only final states close to the initial state are available to an electron, i.e. momentum transfer $\mathbf{q} \approx 0$. This restriction on phase space hinders the energy absorption in forward scattering and enables non-trivial momentum structure of the gap [27], resulting in the observed effects.

We consider the Holstein Hamiltonian on 2D lattice

$$\mathcal{H} = \sum_{\mathbf{k}, \sigma} \xi(\mathbf{k}) c_{\mathbf{k}, \sigma}^\dagger c_{\mathbf{k}, \sigma} + \sum_{\mathbf{q}, \nu} \Omega_\nu \left(b_{\mathbf{q}, \nu}^\dagger b_{\mathbf{q}, \nu} + \frac{1}{2} \right) + \frac{1}{\sqrt{N}} \sum_{\substack{\nu, \sigma \\ \mathbf{k}, \mathbf{q}}} g(\mathbf{k}, \mathbf{q}) c_{\mathbf{k}+\mathbf{q}, \sigma}^\dagger c_{\mathbf{k}, \sigma} \left(b_{\mathbf{q}, \nu} + b_{-\mathbf{q}, \nu}^\dagger \right). \quad (1)$$

Here, $\xi(\mathbf{k})$ nearest neighbor tight-binding energy dispersion measured relative to the chemical potential, $c_{\mathbf{k}}^\dagger, c_{\mathbf{k}}$ ($b_{\mathbf{q}}^\dagger, b_{\mathbf{q}}$) are the standard creation and annihilation operators for an electron (phonon), $g(\mathbf{k}, \mathbf{q})$ is the momentum-dependent e -ph coupling constant, and Ω_ν is the frequency for the Einstein phonon mode ν . Here we take an effective-minimal model to capture the distinctive features of the forward scattering. Although FeSe monolayers are quite complicated (e.g. in their multiband nature), we assume the forward scattering mechanism to be dominant and ignore further complications. This is sufficient to test the forward scattering mechanism.

TABLE I. Parameters used in the simulation

Parameters	Isotropic	Forward
Phonon frequency ($\Omega_{1,2}$)	0.2, 0.001 eV	0.2, 0.05 eV
Phonon coupling ($g_{1,2}^2$)	0.12, 0.001 eV	0.034, 0.01 eV
Band parameters	$V_{nn} = 0.25$ eV, $\mu = 0.0$ eV	
Temperature	≈ 83 K	
Pump pulse	$\omega_p = 1.5$ eV, $\sigma_p = 8$ [1/eV]	
Probe pulse	$\sigma = 25$ [1/eV]	

The superconducting state is modeled by the standard two-particle Nambu spinors in the self-consistent Migdal-Eliashberg formalism and time evolution is done by solving the Gor'kov equations self-consistently on the Keldysh contour [28] with an ultrafast pump field, included via Peierls' substitution. We consider two types of e -ph interactions: an isotropic coupling with $g(\mathbf{k}, \mathbf{q}) = g$, a constant, and a *forward scattering* interaction where $g(\mathbf{k}, \mathbf{q})$ is taken in the limit of perfect forward scattering $g(\mathbf{k}, \mathbf{q}) = g\delta_{\mathbf{q}, \mathbf{0}}$ [27] to reduce the computational cost. The different coupling strengths are tuned to get approximately same superconducting gap ($\Delta \sim 51$ meV) for both isotropic and forward focused interactions (see Supplemental Material). For completeness, we include a solution in the d -wave channel as well.

The nature of the *perfect* forward scattering restricts the system's ability to absorb any energy via scattering processes. Realistically, the coupling has some finite width [10, 24, 29], and there are additional phonons to scatter from in the system. To account for these effects,

we include a second isotropically coupled phonon in the system, whose coupling is weak enough that it can dissipate energy but does not significantly contribute to the superconductivity. Table I lists the parameters used in the simulation.

First, we compare the effect of the pump pulse on the superconductor through the single-particle electron spectral function. Figure 2 displays the calculated time-resolved and angle-resolved photoemission spectroscopy (tr-ARPES) spectra of an *s*-wave superconductor for both types of scattering. For isotropic scattering (the top panels) the equilibrium band structure in normal state (Fig. 2a) shows a kink at the phonon energy ($\pm\Omega_1$), which is common for strong coupling to phonon in the system [30]. The normal state band structure for the forward focused case (Fig. 2e) exhibits different behavior [12]; most notably there is a replica band below the main band, similar to the experimentally observed [10, 15, 31] features of the FeSe monolayer superconductors that have been explained by forward scattering from phonons. The band is flatter in the vicinity of E_F due to the perfect forward scattering limit [27].

The remaining panels in Fig. 2 show the tr-ARPES spectra in the superconducting state, where a pump pulse of amplitude $A_{\max} = 1.2$ [V/ a_0] is used to drive the system along the (11) direction. This fluence is high enough to melt the superconducting order significantly for isotropic pairing [28], as shown in Fig. 2 c,d. The superconducting state in equilibrium is shown in Fig. 2b. The spectra show the characteristics of a strong-coupling superconductor: a decrease of spectral weight near E_F indicating the opening of a gap, the appearance of a particle-hole symmetric shadow band, and a shift of the kink by the maximum gap value [32, 33]. When the pulse hits the system at $t_{\text{delay}} = 0$ [1/eV] (Fig. 2c), the spectral weight redistributes itself along (11) direction. The movement of spectral weight towards E_F represents the melting of the superconducting order. After the pump (Fig. 2d), we observe that the superconducting order has partially melted, as the spectral weight is enhanced near E_F . The spectrum suggests that the system has entered the normal state; however, superconductivity is still present [28], as we will show in the next section.

Figure 2f shows the contrasting case of the superconducting state in the forward scattering scenario. We observe a flattening of the band near E_F compared to the normal state (Fig. 2e). Figs. 2g and 2h show the spectrum when the same pump pulse as used in the isotropic scattering case drives the system. We observe a weaker redistribution of the spectral weight, even for times after the pump (Fig. 2h), indicating that the superconducting order based on forward-focused pairing is remarkably robust and persistent.

To gain further insight we examine the evolution of the spectral gap in the time-domain, which is estimated from

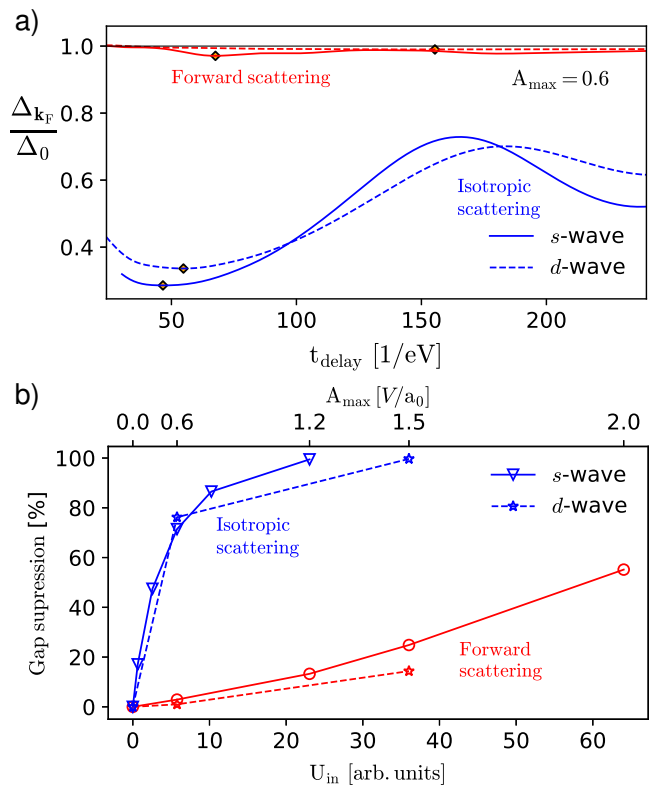


FIG. 3. (Color online) The effect of the pump on the superconducting order parameter. Panel a displays the maximum order parameter (at the Fermi momentum $\mathbf{k} = (\pi/2, \pi/2)$ for *s*-wave, and at $\mathbf{k} = (\pi, 0)$ for *d*-wave) as a function of delay time for fluence $A_{\max} = 0.6$ [V/ a_0]. The *s*-wave and *d*-wave pairing symmetries are compared for both type of scattering. The order parameter is normalized by the equilibrium value Δ_0 (~ 51 meV). The diamond marker indicates the maximum suppression of the superconducting order. Panel b shows the maximum suppression of the superconducting order as a function of incident energy (and fluence top X-axis).

the retarded anomalous self energy $\Sigma_F^R(\mathbf{k}; t, t')$

$$\Delta_{\mathbf{k}}(t_{\text{delay}}, \omega_{\text{rel}} = 0) = \int dt_{\text{rel}} \Sigma_F^R(\mathbf{k}; t_{\text{delay}}, t_{\text{rel}}), \quad (2)$$

where a Wigner transformation $t_{\text{delay}} = \frac{t+t'}{2}$, $t_{\text{rel}} = t - t'$ is used to transform the reference frame to average and relative times. First we calculate the order parameter at the Fermi momentum $\Delta(t_{\text{delay}}) \equiv \Delta_{\mathbf{k}=\mathbf{k}_F}(t_{\text{delay}})$ for both types of scattering; see Fig. 3a which shows $\Delta(t_{\text{delay}})$ for different pairing symmetries after normalizing by the equilibrium value Δ_0 . We observe that the forward scattering Δ melts less than the isotropic scattering Δ . To quantify the suppression we determine the minimum value of the transient order parameter and plot it as function of fluence and absorbed energy in Fig. 3b (a calculation of the energy absorption may be found in the Supplement). Since less energy is absorbed when forward scattering is the dominant source of scattering, a superconducting order built from forward scattering pairing

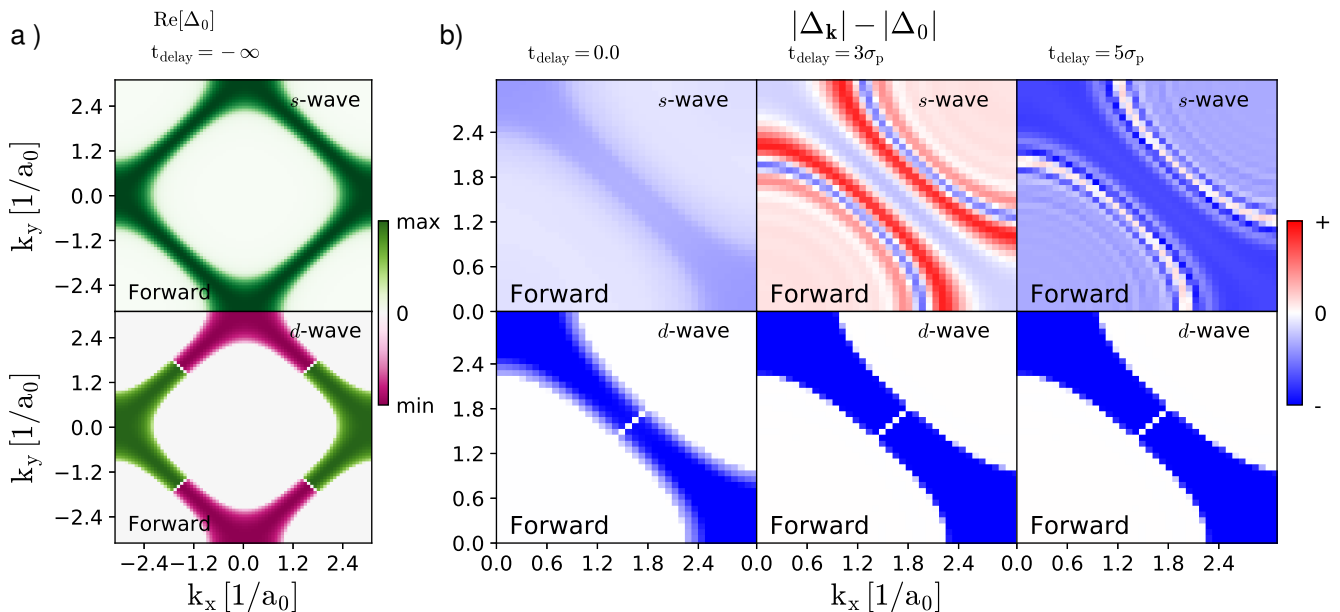


FIG. 4. (color online) The momentum resolved dynamics of the s , d -wave superconducting order for the forward scattering. Panel **a** displays the equilibrium superconducting state. Panel **b** shows the change in magnitude of the superconducting order parameter at three delay times ($0, 3\sigma_p, 5\sigma_p$) when a pump drives the system out of equilibrium.

will also be affected less. Also, we observe that after the pump Δ relaxes in an oscillatory fashion (Fig. 3a). These amplitude mode, or Higgs mode oscillations have been proposed and seen before in literature [28, 34–37] for pumped superconductors. In forward scattering, we observe similar oscillations for low fluences.

Finally, we analyze the momentum structure of the order parameter $\Delta_{\mathbf{k}}(t_{\text{delay}})$. Isotropic scattering pairing and forward scattering pairing result in *momentum independent* and *momentum dependent* s/d -wave order parameters, respectively [12, 27]. By momentum dependence, we mean on top of their respective s/d symmetries. We study the evolution of the forward scattering driven momentum dependent gap for s -wave and d -wave pairing. Figure 4a shows the magnitude of $\Delta_{\mathbf{k}}$ in equilibrium. Although the order parameter is s/d -wave (A_{1g}/B_{1g}), it is not uniform across the Brillouin zone due to the forward focus in the interaction [27]. Figure 4b shows the change in the transient order parameter when the system is driven out of equilibrium by a pump of amplitude $A_{\text{max}} = 1.5$ [V/ a_0].

For s -wave pairing, $\Delta_{\mathbf{k}}$ is suppressed the most at E_F (third snapshot in Fig. 4b at $t_{\text{delay}} = 5\sigma_p$). Surprisingly, in some regions of the Brillouin zone, the order parameter increases when the pump is active (second snapshot in Fig. 4b at $t_{\text{delay}} = 3\sigma_p$). However, overall change in the order parameter is negative because the system absorbs finite amount of energy which leads to dissociation of the Cooper pairs. For d -wave pairing, the superconducting gap does not show any enhancement after the pump and is suppressed at all \mathbf{k} points. To analyze the dynamics

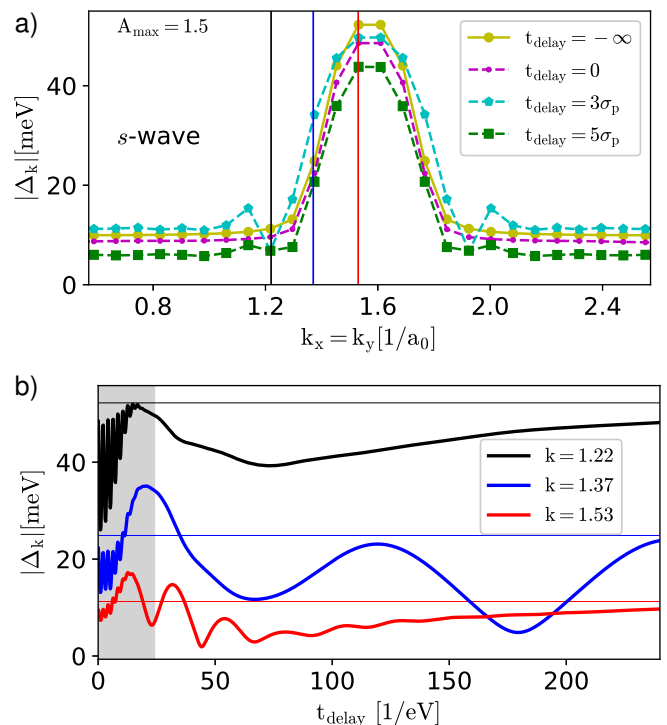


FIG. 5. (Color online) Panel **a** shows magnitude of the s -wave superconducting order along the symmetry line $k_x = k_y$ for different delay times. Panel **b** displays magnitude of the order parameter at three fixed \mathbf{k} points, marked by the vertical straight lines in panel **a**, as a function of delay time. Horizontal straight lines in panel **b** are the equilibrium value for each momentum point, respectively.

further we show the order parameter for s -wave gap as a function of \mathbf{k} along the (11) direction for different delay times in Fig. 5a. Figure 5b displays magnitude of the order parameter as a function of delay time for three representative \mathbf{k} points marked by the vertical lines in Fig. 5a, which highlights the nonuniform changes in $\Delta_{\mathbf{k}}$. Such order suppression is characteristically different in isotropic interaction scenario, where the suppression is larger and momentum independent, shown in Fig. 3.

In summary, we have studied the effect of e -ph scattering focused in the forward direction on the superconducting state in the time-domain and compared our results with isotropic scattering case. The forward scattering superconductor shows a robust, persistent superconducting order against the pump-induced perturbations. We also observe a momentum structure of the superconducting order parameter in the forward scattering. The order parameter exhibits a non-uniform melting in momentum space in the non-equilibrium state. These characteristic features of the forward scattering are in direct contrast with the conventional BCS isotropic superconductors, where a reasonable fluence can melt the superconducting order and the suppression of the superconducting order shows no momentum dependence. In fact, even unconventional (cuprate) superconductors show a rapid suppression of the gap for weak pump pulse [38]. We explain our results for the forward pairing superconducting order using the restriction of phase space available for the scattering process to occur, which results in less absorption of energy. We support our explanation by estimating the absorbed energy and studying the dynamics of the superconducting order parameter in the time domain. These distinctive features of forward scattering may be detectable using momentum-resolved experiments such as time-resolved ARPES.

Recent work has suggested a weak forward scattering phonon as a source of the high T_C as an enhancement of an unconventional pairing mechanism. In this scenario, the time-resolved signatures discussed here would appear essentially identical to a standard BCS superconductor since the lack of phase space does not apply, and a quantitative comparison would have to be made with respect to some reference material; an FeSe intercalate which has no interfacial phonons may be used for an absolute comparison to see if there is an increase in energy absorption commensurate with the enhanced pairing.

ACKNOWLEDGMENTS

We acknowledge fruitful discussion with Doug Scalapino, Yan Wang, Louk Rademaker, Avinash Rustagi and Omadillo Abdurazakov. This research used resources of the National Energy Research Scientific Computing Center, a DOE Office of Science User Facility supported by the Office of Science of the U.S. Department

of Energy under Contract No. DE-AC02-05CH11231.

* akumar13@ncsu.edu

† akemper@ncsu.edu

- [1] D. Liu, W. Zhang, D. Mou, J. He, Y.-B. Ou, Q.-Y. Wang, Z. Li, L. Wang, L. Zhao, S. He, Y. Peng, X. Liu, C. Chen, L. Yu, G. Liu, X. Dong, J. Zhang, C. Chen, Z. Xu, J. Hu, X. Chen, X. Ma, Q. Xue, and X. J. Zhou, *Nature Communications* **3**, ncomms1946 (2012).
- [2] W. Qing-Yan, L. Zhi, Z. Wen-Hao, Z. Zuo-Cheng, Z. Jin-Song, L. Wei, D. Hao, O. Yun-Bo, Deng Peng, C. Kai, W. Jing, S. Can-Li, H. Ke, J. Jin-Feng, J. Shuai-Hua, W. Ya-Yu, W. Li-Li, C. Xi, Ma Xu-Cun, and X. Qi-Kun, *Chinese Physics Letters* **29**, 037402 (2012).
- [3] S. He, J. He, W. Zhang, L. Zhao, D. Liu, X. Liu, D. Mou, Y.-B. Ou, Q.-Y. Wang, Z. Li, L. Wang, Y. Peng, Y. Liu, C. Chen, L. Yu, G. Liu, X. Dong, J. Zhang, C. Chen, Z. Xu, X. Chen, X. Ma, Q. Xue, and X. J. Zhou, *Nature Materials* **12**, 605 (2013).
- [4] I. I. Mazin, D. J. Singh, M. D. Johannes, and M. H. Du, *Physical Review Letters* **101**, 057003 (2008).
- [5] V. Mishra, D. J. Scalapino, and T. A. Maier, *Scientific Reports* **6**, srep32078 (2016).
- [6] A. Linscheid, S. Maiti, Y. Wang, S. Johnston, and P. Hirschfeld, *Physical Review Letters* **117**, 077003 (2016).
- [7] X. Chen, S. Maiti, A. Linscheid, and P. J. Hirschfeld, *Physical Review B* **92**, 224514 (2015).
- [8] J. Kang and R. M. Fernandes, *Physical Review Letters* **117**, 217003 (2016).
- [9] S. Coh, M. L. Cohen, and S. G. Louie, *New Journal of Physics* **17**, 073027 (2015).
- [10] J. J. Lee, F. T. Schmitt, R. G. Moore, S. Johnston, Y.-T. Cui, W. Li, M. Yi, Z. K. Liu, M. Hashimoto, Y. Zhang, D. H. Lu, T. P. Devereaux, D.-H. Lee, and Z.-X. Shen, *Nature* **515**, 245 (2014).
- [11] D.-H. Lee, *Chinese Physics B* **24**, 117405 (2015).
- [12] L. Rademaker, Y. Wang, T. Berlijn, and S. Johnston, *New Journal of Physics* **18**, 022001 (2016).
- [13] S. Choi, S. Johnston, W.-J. Jang, K. Koepernik, K. Nakatsukasa, J. M. Ok, H.-J. Lee, H. W. Choi, A. T. Lee, A. Akbari, Y. K. Semertzidis, Y. Bang, J. S. Kim, and J. Lee, *Physical Review Letters* **119**, 107003 (2017).
- [14] Z.-X. Li, F. Wang, H. Yao, and D.-H. Lee, *Science Bulletin* **61**, 925 (2016).
- [15] S. Rebec, T. Jia, C. Zhang, M. Hashimoto, D. Lu, R. Moore, and Z. Shen, *Physical Review Letters* **118** (2017), 10.1103/PhysRevLett.118.067002, arXiv:1606.09358.
- [16] Y. Zhou and A. J. Millis, *Physical Review B* **96**, 054516 (2017).
- [17] I. A. Nekrasov, N. S. Pavlov, and M. V. Sadovskii, arXiv:1707.05262 [cond-mat] (2017), arXiv: 1707.05262.
- [18] J. Jandke, F. Yang, P. Hlobil, T. Engelhardt, K. Zakeri, C. Gao, J. Schmalian, and W. Wulfhekel, arXiv:1710.08861 [cond-mat] (2017).
- [19] Q. Song, T. L. Yu, X. Lou, B. P. Xie, H. C. Xu, C. H. P. Wen, Q. Yao, S. Y. Zhang, X. T. Zhu, J. D. Guo, R. Peng, and D. L. Feng, arXiv:1710.07057 [cond-mat] (2017), arXiv: 1710.07057.

- [20] F. Li and G. A. Sawatzky, *Physical Review Letters* **120**, 237001 (2018).
- [21] S. Zhang, J. Guan, Y. Wang, T. Berlijn, S. Johnston, X. Jia, B. Liu, Q. Zhu, Q. An, S. Xue, Y. Cao, F. Yang, W. Wang, J. Zhang, E. W. Plummer, X. Zhu, and J. Guo, *Physical Review B* **97**, 035408 (2018).
- [22] M. L. Kulić and O. V. Dolgov, *Physica Status Solidi b* **242**, 151 (2004).
- [23] S. Roof, K. Kemp, M. Havey, and I. Sokolov, *Physical Review Letters* **117**, 073003 (2016).
- [24] M. L. Kulić and O. V. Dolgov, *New Journal of Physics* **19**, 013020 (2017).
- [25] N. Bulut and D. J. Scalapino, *Phys. Rev. B* **54**, 14971 (1996).
- [26] A. Aperis, P. Kotetes, G. Varelogiannis, and P. M. Oppeneer, *Phys. Rev. B* **83**, 092505 (2011).
- [27] Y. Wang, K. Nakatsukasa, L. Rademaker, T. Berlijn, and S. Johnston, *Superconductor Science and Technology* **29**, 054009 (2016).
- [28] A. F. Kemper, M. A. Sentef, B. Moritz, J. K. Freericks, and T. P. Devereaux, *Phys. Rev. B* **92**, 224517 (2015).
- [29] Y. Zhou and A. J. Millis, *Physical Review B* **93**, 224506 (2016).
- [30] S. Engelsberg and J. R. J. R. Schrieffer, *Phys. Rev.* **131**, 993 (1963).
- [31] R. Peng, H. C. Xu, S. Y. Tan, H. Y. Cao, M. Xia, X. P. Shen, Z. C. Huang, C. H. P. Wen, Q. Song, T. Zhang, B. P. Xie, X. G. Gong, and D. L. Feng, *Nature Communications* **5**, 5044 (2014).
- [32] M. Eschrig and M. R. Norman, *Physical Review B* **67**, 144503 (2003).
- [33] W. S. Lee, W. Meevasana, S. Johnston, D. H. Lu, I. M. Vishik, R. G. Moore, H. Eisaki, N. Kaneko, T. P. Devereaux, and Z. X. Shen, *Physical Review B* **77**, 140504 (2008).
- [34] B. Nosarzewski, B. Moritz, J. K. Freericks, A. F. Kemper, and T. P. Devereaux, *Physical Review B* **96**, 184518 (2017).
- [35] R. Matsunaga, Y. I. Hamada, K. Makise, Y. Uzawa, H. Terai, Z. Wang, and R. Shimano, *Physical Review Letters* **111**, 057002 (2013).
- [36] R. Matsunaga, N. Tsuji, H. Fujita, A. Sugioka, K. Makise, Y. Uzawa, H. Terai, Z. Wang, H. Aoki, and R. Shimano, *Science* **345**, 1145 (2014).
- [37] Y. Murakami, P. Werner, N. Tsuji, and H. Aoki, *Physical Review B* **93**, 094509 (2016).
- [38] J. Graf, C. Jozwiak, C. L. Smallwood, H. Eisaki, R. A. Kaindl, D.-H. Lee, and A. Lanzara, *Nature Physics* **7**, 805 (2011).